Journal of Chromatography A, 1217 (2010) 660–666

Contents lists available at ScienceDirect

Journal of Chromatography A

journal homepage: www.elsevier.com/locate/chroma

Understanding and mitigating conductivity transitions in weak cation exchange chromatography

Jace Fogle*, Jenny Hsiung

Genentech Process Research and Development, 1 DNA Way MS 75A, South San Francisco, CA 94080, USA

ARTICLE INFO

Article history:
Received 18 May 2009
Received in revised form 7 November 2009
Accepted 30 November 2009
Available online 4 December 2009

Keywords:
Weak cation exchange chromatography
CM Ceramic HyperD
CM Sepharose Fast Flow
Conductivity transitions
pH shift
Counterions

ABSTRACT

Large conductivity fluctuations were observed during a high pH wash step in a weak cation exchange chromatography process. These conductivity transitions resulted in a conductivity drop during pH increase and a conductivity rise during pH decrease. In some cases, the absolute conductivity change was greater than 6 mS/cm which was sufficient to affect target protein retention on the column. Further investigation revealed that wash buffer concentration, resin ligand density, and resin ligand pK have a profound effect on the magnitude of the conductivity transitions and the shape of corresponding pH traces. A potentiometric electrode selective for sodium ions was used to measure effluent counterion concentrations from two preparative resins during high pH washes, and the number of exchangeable counterions was compared to predictions made using ion exchange equilibrium theory. Results from this analysis show that conductivity transitions can be effectively mitigated without compromising process performance by optimizing the trade-off between wash buffer concentration and wash phase duration.

1. Introduction

Weak cation exchange resins have been widely employed for the chromatographic capture and polishing of both naturally occurring and recombinant proteins [1–9]. These resins are typically functionalized with carboxylic acid (COOH) groups that are deprotonated at intermediate and high pH. These functional groups are often referred to as carboxymethyl, or "CM", groups when the acid moiety is attached to the resin base matrix through a linker containing a methylene group adjacent to the carboxylic acid group. This is in contrast to so-called strong cation exchange resins which generally carry sulfonate (SO_3^-), or "S", functional groups that are protonated only at very low pH. The classification of CM and S resins as "weak" and "strong", respectively, follows from the fact that S groups are deprotonated over a wider pH range than CM groups. Protein retention on strong cation exchange resins is usually greater than on weak cation exchangers with identical base matrices [10]. However, there have been instances where the opposite trend was observed [11,12]. Further, some researchers have demonstrated that hydrophobic interactions play a significant role in retention on cation exchange, and that the hydrophobic contribution to retention on equivalent weak and strong cation exchange resins can be very different at high salt concentration [13,14]. In some separation processes, a CM resin may provide better selectivity because the difference in retention of the target protein and contaminant proteins is maximized. If the CM resin employed also provides high ligand density, then the sorbent may provide enhanced binding capacity and salt-tolerance along with favorable selectivity. One of the CM resins employed in this study, CM Ceramic HyperD, was evaluated with these considerations in mind.

However, it has been reported that the use of weak cation exchange resins can be complicated by the fact that transient changes in pH may accompany sudden shifts in salt concentration such as those that are used to elute target proteins [15–18]. For instance, an unwanted, temporary pH decrease was observed during a high salt protein elution step even though both the high and low salt mobile phases were buffered at the same pH. This pH transition was attributed to the exchange of protons for positively charged buffer counterions on the resin during the salt increase [16]. Since bind-and-elute cation exchange chromatography steps are routinely operated near the pK of carboxylic acid groups, these issues are anticipated to be more pronounced when working with weak cation exchange resins.

Here, we observed that significant conductivity transitions may result from step changes in pH on weak cation exchange resins. This occurred during development of a high pH wash intended for selective removal of host cell proteins prior to elution of a recombinant monoclonal antibody. The initial increase in pH was accompanied by an unexpected, temporary decrease in conductivity, and the subsequent decrease in pH was accompanied by a temporary increase in conductivity. This occurred even when the counterion (sodium) concentrations of the low pH and high pH wash buffers

* Corresponding author. Tel.: +1 650 467 4087; fax: +1 650 225 4049.
E-mail address: fogle.jace@gene.com (J. Fogle).

0021-9673/$ – see front matter © 2009 Elsevier B.V. All rights reserved.
doi:10.1016/j.chroma.2009.11.099

were matched. Blank runs in the absence of protein confirmed that this effect was indeed related to the behavior of the resin and was not the result of protein elution at elevated pH. Further, this effect was not limited only to a particular resin.

It has been shown that conductivity transitions can result from step increases in pH on a strong S-type cation exchange resin that also contains weak acid CM groups [19]. This result was consistent with a local equilibrium model that predicted a decrease in counterion concentration at the outlet of the column. However, this analysis did not include a direct comparison of experimental and theoretical counterion profiles.

In this study, we investigated the effects of resin properties such as ligand density and pK and process conditions such as wash buffer concentration on the magnitude of conductivity transitions during high pH washes. We used a potentiometric electrode selective for sodium ions in an effort to measure effluent counterion concentrations directly and determine the total number of exchangeable counterions during high pH washes. As anticipated, high ligand density led to more exchange of counterions and conductivity transitions of greater magnitude. Thus, the practical benefits provided by high ligand density may require adoption of strategies to mitigate conductivity transitions. An understanding of these relationships and their effect on conductivity transitions could potentially save process developers a great deal of time on empirical optimization experiments.

An additional objective of this work was to determine whether the observed conductivity transitions could be mitigated or eliminated by using a pH gradient in place of the step change. In this case, we tested the efficacy of a relatively short gradient that would be amenable to implementation in a large-scale purification process.

1.1. Ion exchange equilibrium theory

The number of counterions changing phase upon a pH shift (N_{Na^+}) can be calculated from the difference in the concentration of deprotonated CM groups in the adsorbed phase (q_{Na^+}) at high pH and low pH:

$$N_{Na^+} = \left(q_{Na^+}^{\text{high pH}} - q_{Na^+}^{\text{low pH}}\right) \cdot V \tag{1}$$

Here the adsorbed phase concentrations are in units of moles per liter of packed bed and V is the bed volume. In this case, N_{Na^+} is expressed in moles. The number of counterions desorbing from the resin upon pH decrease should be equal to the number of counterions adsorbing to the resin upon a pH increase for the equal but opposite change in pH.

q_{Na^+} is related to the dissociation constant of the CM group (K), the total concentration of CM ligands on the resin (q_R), the solution phase concentration of sodium ions (C_{Na^+}), and the solution phase concentration of H^+ ions (C_{H^+}) [17,20]:

$$K = \frac{{q_{Na^+}}^2 C_{H^+}}{(q_R - q_{Na^+})\, C_{Na^+}} \tag{2}$$

which can be re-arranged to:

$${q_{Na^+}}^2 C_{H^+} + q_{Na^+} K C_{Na^+} - K q_R C_{Na^+} = 0 \tag{3}$$

Application of the quadratic formula yields:

$$q_{Na^+} = \frac{1}{2}\left[\frac{-KC_{Na^+} + \sqrt{(KC_{Na^+})^2 + 4KC_{Na^+}C_{H^+}q_R}}{C_{H^+}}\right] \tag{4}$$

For a chromatography column at equilibrium, C_{H+} and C_{Na^+} are calculated directly from the pH and counterion concentration of the mobile phase buffer. Thus, K and q_R are the only constants needed to perform a balance on counterions from one steady-state set of buffer conditions to another.

K and q_R can be estimated by fitting a theoretical resin titration curve based on Eq. (4) to an experimental resin titration curve. In this process, an experimental value of q_{Na^+} is calculated from a mass balance on sodium ions in the resin slurry being titrated:

$$q_{Na^+} = \frac{m_{Na^+} - C_{Na^+}(V_o + (m_{Na^+}/N)) + C_{Na^+}^{\text{init}} V_o}{V} \tag{5}$$

Here, m_{Na^+} is the moles of NaOH titrant added to the resin slurry, N is the normality of the titrant, V_o is the initial volume of resin slurry, and $C_{Na^+}^{\text{init}}$ is the initial concentration of sodium chloride in the resin slurry. The value of C_{Na^+} is calculated from the solution phase electroneutrality condition:

$$C_{Na^+} + C_{H^+} = C_{Cl^-} + C_{OH^-} \tag{6}$$

Eq. (6) can be re-arranged to solve explicitly for C_{Na^+}:

$$C_{Na^+} = C_{Cl^-} + \frac{K_W}{10^{-\text{pH}}} - 10^{-\text{pH}} \tag{7}$$

where K_W is the dissociation constant of water and C_{Cl^-} is equal to $C_{Na^+}^{\text{init}}$ after adjusting for volume change due to titrant addition. Best-fit values of K and q_R can then be regressed through sum of least-squares analysis. In this study, the difference in theoretical (Eq. (4)) and experimental (Eq. (5)) values of q_{Na^+} across the entire titration curve was minimized.

2. Materials and methods

2.1. Resins and columns

Experiments were performed on CM Ceramic HyperD, S Ceramic HyperD (Pall Corporation, East Hills, NY) and CM Sepharose FF (GE Healthcare, Piscataway, NJ) cation exchange resins. For column chromatography experiments, the resins were packed into 0.66 cm i.d. × 20 cm Omnifit columns (Bio-Chem Valve, Inc., Cambridge, England).

2.2. Dynamic binding capacity measurements

The resin dynamic binding capacities at 1% breakthrough ($DBC_{1\%}$) were measured using a full-length monoclonal antibody. In this case, the resins were evaluated for direct antibody capture from harvested cell culture fluid. Measurements were made using an AKTA Explorer 100 FPLC (GE Healthcare, Piscataway, NJ). For purposes of this study, 1% breakthrough was defined as the column load density (grams of antibody loaded per liter of packed bed) at which antibody concentration in the column effluent was equal to one percent of the antibody concentration in the load.

Flow rates were selected based on manufacturer recommendations and known pressure limitations at manufacturing scale. CM Ceramic HyperD was loaded at a linear velocity of 600 cm/h, and CM Sepharose FF was loaded at 200 cm/h.

Full-length monoclonal antibodies were expressed in Chinese hamster ovary (CHO) cells in 250 or 400 L bioreactors at Genentech (South San Francisco, CA). Cell culture fluid was harvested using depth filtration and sterile filtration. Harvested cell culture fluid (HCCF) was adjusted to pH 5.5 by adding 1.0 M acetic acid. HCCF conductivity was adjusted to 6 mS/cm by adding purified water. Conditioned HCCF was sterile filtered prior to column loading.

Column effluent was collected in 15 mL fractions, and the concentration of antibody in the fractions was quantified with an HPLC assay using a POROS Protein A (2.1 mm × 30 mm) affinity column (cat. No. 1-5024-12) from Applied Biosystems (Foster City, CA). The column was run at 2.0 mL/min at ambient temperature for a duration of 6 min. The column was equilibrated with phosphate-buffered saline (PBS) at pH 7.2. Samples were injected without dilution and antibody was eluted with PBS adjusted to pH 2.0 (with

Table 1
pH shift buffer components (in mM).

MOPS buffers	50 mM	100 mM	200 mM	300 mM
Na^+ MOPS (mM)	33	66	132	198
MOPS acid (mM)	17	34	68	102
NaCl (mM)	40	25	0	0
Measured conductivity (mS/cm)	6.30	6.54	7.48	10.47
Measured pH	7.33	7.37	7.42	7.46
MES buffers	**50 mM**	**100 mM**	**200 mM**	**300 mM**
Na^+ MES (mM)	10	19	39	58
MES acid (mM)	40	81	161	242
NaCl (mM)	50	50	40	33
Measured conductivity (mS/cm)	6.00	6.50	6.31	6.40
Measured pH	5.43	5.46	5.46	5.48

6N HCl). Absorbance was monitored at 280 nm and the elution peak was integrated. The concentration of antibody was then calculated using a standard curve generated with purified antibody.

2.3. Column chromatography—high pH washes and conductivity transitions

2.3.1. Step changes in pH in the presence of antibody

The CM Ceramic HyperD column was initially equilibrated with five column volumes (CV) of a low pH buffer (300 mM MES, 20 mM NaCl, pH 5.5). Antibody (adjusted to approximately pH 5.5 and 6 mS/cm as described in Section 2.2) was then loaded on the column to a density of 70 mg of antibody per milliliter of column bed volume. The column was washed with eight CV of the low pH buffer followed by eight CV of a high pH buffer (100 mM MOPS, 10 mM NaCl, pH 7.0). The column was re-equilibrated with eight CV of the low pH buffer. Finally, antibody was eluted with a step increase in salt concentration to 500 mM acetate, pH 5.5. The flow rate during column equilibration and load was 600 cm/h, while the flow rate during the washes was 200 cm/h.

NaCl was added to the wash buffers to maintain the conductivity above 4 mS/cm. The manufacturer of CM Ceramic HyperD recommends maintaining the conductivity of all buffers at or above approximately 4 mS/cm. This recommendation is related to the morphology of the sorbent bead, a composite in which a ligand-bearing hydrogel is polymerized within the macropores of a rigid ceramic bead. Due to the high ligand density on the hydrogel, use of mobile phase having conductivity less than approximately 4 mS/cm can lead to swelling of the hydrogel, particularly that which is near the surface of the bead. While this swelling is expected to be reversible, buffer conditions were chosen in an effort to optimize the pressure-flow characteristics of the resin in this work.

2.3.2. Variation of wash buffer conductivities (in the absence of antibody)

Initial experiments were performed on CM Ceramic HyperD and CM Sepharose FF. The columns were equilibrated with five CV of a low pH buffer (300 mM MES, 33 mM NaCl, pH 5.5). The column was then washed with a high pH buffer (100 mM MOPS, 25 mM NaCl, pH 7.5) until the pH stabilized at the higher value. Finally, the column was re-equilibrated by switching back to the low pH buffer until pH and conductivity traces were stable. Note that the counterion concentrations (Na^+) of the low pH buffer and the high pH buffer were equivalent in this case. This was accomplished by adjusting the NaCl concentration in each buffer such that the sum of the NaCl concentration and the buffer concentration in the sodium form were equal in the two buffers. The total counterion concentration in the buffers was 91 mM (see Table 1). Both columns were run at 200 cm/h.

Additional experiments were performed with CM Ceramic HyperD at varying buffer concentrations. The column was equilibrated with five CV of a low pH buffer (50 mM, 100 mM, 200 mM, or 300 mM MES, pH 5.5). The column was then washed with a high pH buffer (50 mM, 100 mM, 200 mM, or 300 mM MOPS, pH 7.5) until the effluent pH reached 7.1. At that point, the high pH wash was continued for an additional three CV to stabilize pH before switching back to the low pH buffer. When the effluent pH dropped below 5.8, the run was allowed to continue for an additional four CV to completely re-equilibrate the column. The flow rate was constant at 200 cm/h for all four runs. Table 1 summarizes the components of each buffer along with the measured conductivity and pH.

2.3.3. pH gradient in the presence of antibody

The CM Ceramic HyperD column was initially equilibrated with five CV of a low pH buffer (300 mM MES, 20 mM NaCl, pH 5.5). Antibody (adjusted to approximately pH 5.5 and 6 mS/cm as described in Section 2.2) was then loaded on the column to a density of 70 mg of antibody per milliliter of column bed volume. The column was then washed with eight CV of the low pH buffer followed by eight CV of a high pH buffer (100 mM MOPS, 10 mM NaCl, pH 7.0). When the high pH wash was complete, a 10 CV linear gradient was run from 0 to 100% with respect to low pH buffer concentration. Following the pH gradient, the column was washed with an additional two CV of the low pH buffer to ensure complete re-equilibration. Finally, antibody was eluted with a step increase in salt concentration to 500 mM acetate, pH 5.5. The flow rate during column equilibration and load was 600 cm/h, while the flow rate during the washes and the gradient was 200 cm/h.

2.4. Resin titration curves

Resins were first packed into 0.66 cm i.d. × 20 cm Omnifit columns in order to accurately determine the resin volume (in mL of packed bed) for determination of K and q_R. The columns were equilibrated with 150 mM NaCl adjusted to pH 2.5 with 6N HCl (low pH buffer) so that all functional groups on the resins would be protonated at the beginning of the titration experiment. The columns were then unpacked by removing the bottom adaptor and forcing the resin out of the column under flow provided by an AKTA Explorer 100 FPLC. The resin slurries were titrated with a standard solution of 1N NaOH solution from pH 2.5 to 6.5.

Theoretical resin titration curves were fit to the experimental data as described in Section 1.1.

2.5. Offline measurement of pH and Na^+ concentration

The CM Ceramic HyperD and CM Sepharose FF columns were initially equilibrated with five CV of a low pH buffer (300 mM MES, 33 mM NaCl, pH 5.5). The column was then washed with a high pH buffer (100 mM MOPS, 25 mM NaCl, pH 7.5) until the pH stabilized at the higher value. Finally, the column was re-equilibrated by switching back to the low pH buffer until pH and conductivity traces were stable. For each resin, the column effluent was collected in fractions equal to 0.5 CV. The flow rate during all washes was 200 cm/h.

The pH and Na^+ concentration of each fraction was measured with a BioProfile 400 analyzer (Nova Biomedical Corporation, Waltham, MA). The BioProfile 400 analyzer contains a potentiometric electrode that is selective for Na^+ ions and accurate in the range of 40–220 mM (manufacturer estimate). The BioProfile analyzer was calibrated at a sodium ion concentration of 140 mM immediately prior to use.

3. Results and discussion

CM Ceramic HyperD provided significantly higher dynamic binding capacity than S Ceramic HyperD or CM Sepharose FF for the

Table 2
Dynamic binding capacities of weak cation exchange resins used for capture of a monoclonal antibody from cell culture fluid.

Resin	DBC at 1% breakthrough[a]	Manufacturer ionic capacity range [21,23]	Linear flow rate
CM Ceramic HyperD	89 g/L	>250 meq/L	600 cm/h
S Ceramic HyperD	27 g/L	≥150 meq/L	600 cm/h
CM Sepharose FF	48 g/L	90–130 meq/L	200 cm/h

[a] *Note*: The units of DBC are grams per liter of packed bed.

monoclonal antibody of interest in this study (Table 2). Presumably, this is due to the resin's high ligand density and fast mass transfer rates characteristic of homogeneous diffusion through pores filled with functionalized hydrogel [21,22]. Moreover, the incompressible ceramic base matrix unique to CM Ceramic HyperD facilitated much faster flow rates than the agarose-based CM Sepharose FF. These properties offer potentially valuable opportunities for improvement in both facility fit and cycle time during process scale-up.

However, approximately 37% of the antibody desorbed and eluted from the CM Ceramic HyperD column during the high pH wash prior to the elution phase. Surprisingly, this did not occur during the initial pH increase to 7.0; rather, the yield loss was observed as the pH was decreased to 5.5 at the end of the high pH wash phase. Upon closer inspection of the lab scale chromatograms, it became apparent that the undesired antibody desorption coincided with a transient increase in conductivity to almost 10 mS/cm (Fig. 1). While step changes in salt concentration are known to cause transient pH fluctuations in weak ion exchangers (and in fact this was observed here during the elution phase of the run), it was unclear whether a conductivity transition of this magnitude could be caused solely by counterion exchange on the resin.

To better understand the nature of the conductivity fluctuations observed during the high pH wash, experiments were performed on two resins in the absence of protein (Fig. 2). Very large conductivity transitions were observed during both the stepwise increase in pH and the stepwise decrease in pH on CM Ceramic HyperD, consistent with the behavior of the resin when loaded with protein. Conductivity transitions were also observed on the alternate resin, CM Sepharose FF, although the absolute changes in conductivity during the high pH wash were much smaller. In both cases, the transient changes in conductivity occurred despite the fact that the counterion concentrations in the low pH and the high pH buffer were matched (see Section 2.3.2). While the magnitudes of the conductivity transitions on CM Sepharose FF were fairly consistent with those reported by Pabst et al. [19], the magnitudes of the conductivity transitions on CM Ceramic HyperD were much larger.

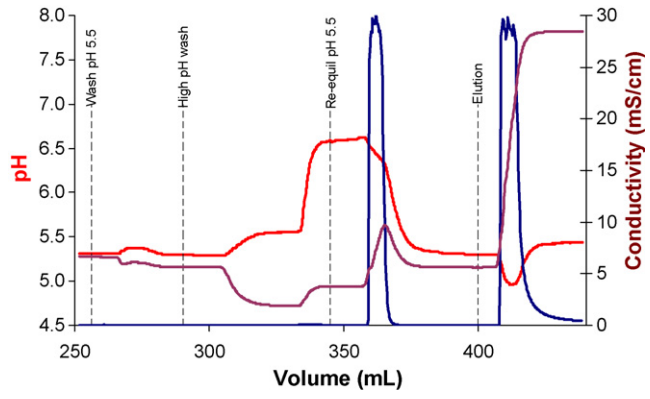

Fig. 1. Screening experiment with mAb on CM Ceramic HyperD. The blue trace is UV absorbance at 280 nm, the brown trace is conductivity, and the red trace is pH. (For interpretation of the references to color in this figure legend, the reader is referred to the web version of the article.)

It was also noticed that a pronounced shoulder was present on the leading edge of the pH profile for CM Ceramic HyperD, and a smaller shoulder was present on the trailing edge of the profile. When the concentration of the wash buffers was varied (see Fig. 3), these shouldering effects became more pronounced at lower buffer concentrations and less pronounced at higher buffer concentrations. At the highest buffer concentration (300 mM MES and 300 mM MOPS), the leading edge shoulder is barely visible against the main peak, and the trailing edge shoulder in not seen. The shouldering effect is likely due to counterion exchange on the resin, since desorption of H^+ ions would temporarily buffer the mobile phase against a pH increase (and vice-versa) during the high pH wash. This effect would be expected to diminish at high buffer concentrations, and in fact this is the case. Moreover, this effect was not observed with CM Sepharose FF which has substantially lower ligand density. Unfortunately, the conductivity transitions on CM Ceramic HyperD become more pronounced with larger overall changes in conductivity when more concentrated buffers are used. In this case there is a clear trade-off between the use of low concentration wash buffers that would result in broader, shallower conductivity transitions that might be less likely to result in protein desorption and the use of high concentration wash buffers that would facilitate shorter wash phases and lower

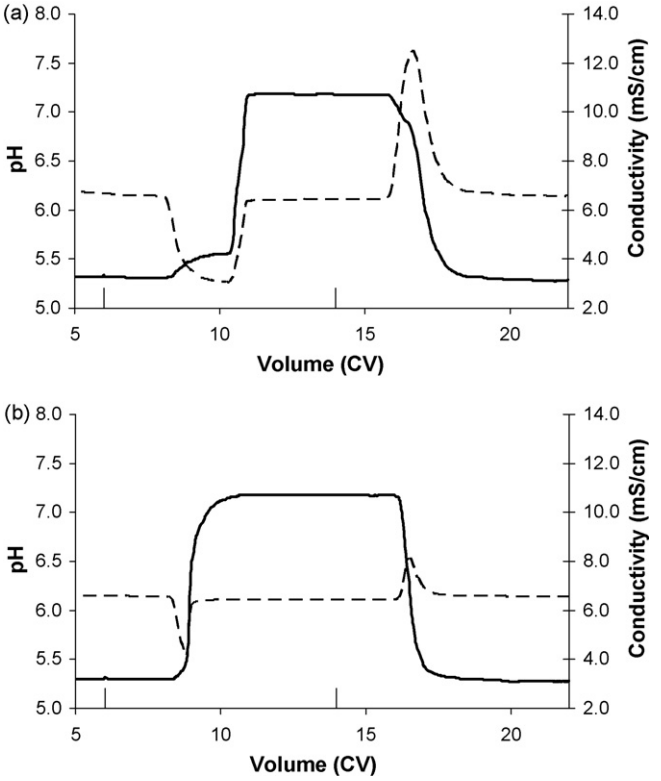

Fig. 2. pH shift experiments with online (AKTA Explorer) conductivity monitoring. Solid lines are pH traces and dashed lines are conductivity traces. The first hash mark along the *x*-axis indicates the transition from low pH buffer (pH 5.5) to the high pH buffer (pH 7.5). The second hash mark along the *x*-axis indicates the transition from high pH buffer back to low pH buffer. (A) CM Ceramic HyperD, (B) CM Sepharose FF.

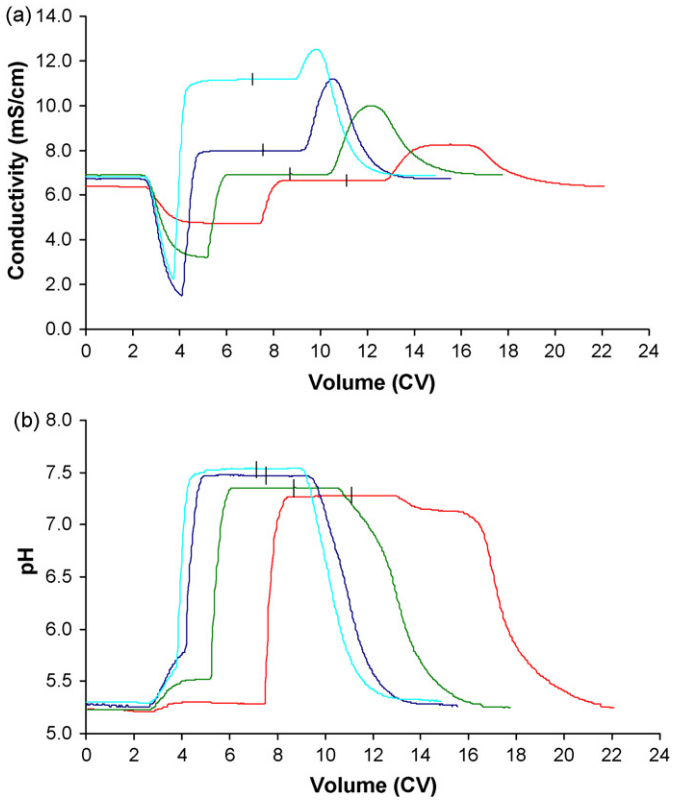

Fig. 3. pH shift experiments on CM Ceramic HyperD using 50 mM MES and MOPS (red traces), 100 mM MES and MOPS (green traces), 200 mM MES and MOPS (dark blue traces), and 300 mM MES and MOPS (light blue traces). The hash marks on each trace indicate the transition from high pH MOPS buffer (pH 7.5) to low pH MES buffer (pH 5.5). (A) Conductivity, (B) pH. (For interpretation of the references to color in this figure legend, the reader is referred to the web version of the article.)

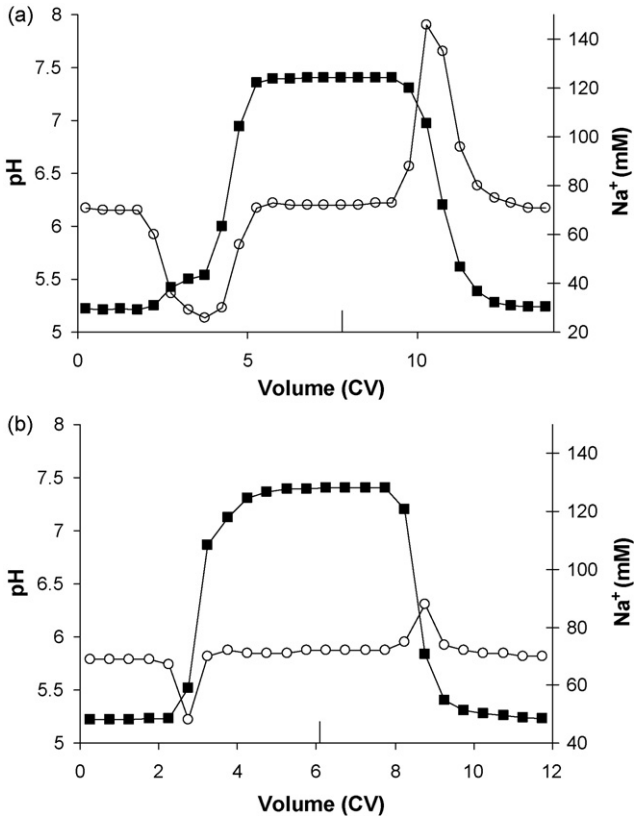

Fig. 5. pH shift experiments with offline (BioProfile 400) ion concentration measurement. The transition between the low pH buffer (pH 5.5) and the high pH buffer occurred at 0 CV. The hash mark along the *x*-axis indicates the transition from high pH buffer back to low pH buffer. (■) Offline pH readings, (○) offline sodium ion concentration measurements. (A) CM Ceramic HyperD, (B) CM Sepharose FF. Lines between data points are for visual purposes only.

buffer volumes but cause conductivity transitions of greater magnitude.

This problem was overcome by implementing a pH gradient in place of the stepwise decrease in pH at the end of the high pH wash (Fig. 4). Using the same buffers, a relatively short gradient (10 column volumes followed by two column volumes of re-equilibration with the low pH buffer) resulted in a much more gradual pH change and almost no transient increase in conductivity above that of the low pH buffer. No desorption of antibody was detected, and the elution phase proceeded as expected. While the use of a gradient wash introduces some additional complexities for implementation

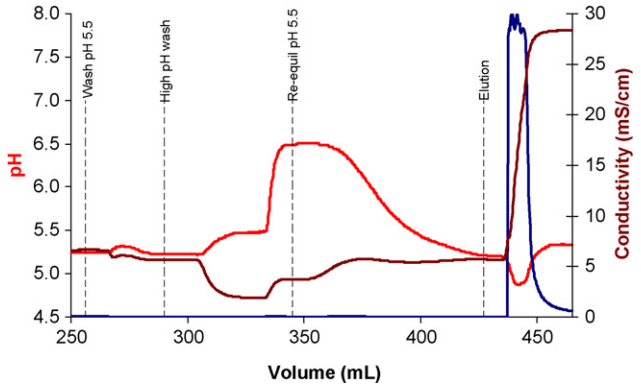

Fig. 4. Screening experiment with mAb on CM Ceramic HyperD using a pH gradient in place of step decrease in pH. The blue trace is UV absorbance at 280 nm, the brown trace is conductivity, and the red trace is pH. (For interpretation of the references to color in this figure legend, the reader is referred to the web version of the article.)

at larger scale, this approach allows for the use of a high capacity weak cation exchanger with a high pH wash for additional host cell protein removal. Further, the gradient slope could be tuned to optimize the trade-off between wash phase duration and target protein retention. Following such optimization, one could determine if the time required for the gradient is offset by the time saved by loading CM Ceramic HyperD at high linear velocity as illustrated in Table 2.

In the future, process developers might benefit from a fast, direct method for measuring counterion concentrations in the effluents of high capacity cation exchange columns. While offline calibration curves can be generated to relate conductivity and counterion concentration, the correlation is typically not linear and it can be difficult to account for the contributions from many different ions. (In this example, MES and MOPS also contribute to conductivity to some extent and they can both be present during high pH washes.) Here, a potentiometric electrode selective for sodium ions was used to verify that the conductivity transitions resulted from exchange of Na^+ ions on and off the resin during pH shifts. For CM Ceramic HyperD, the sodium ion concentration decreased from 70 to 26 mM during a pH increase to 7.5, and the sodium ion concentration increased from 70 to 146 mM during the pH decrease back to 5.5 (Fig. 5A). For CM Sepharose, the sodium ion concentration decreased from 70 to 48 mM during a pH increase to 7.5, and sodium ion concentration increased from 70 to 88 mM during the pH decrease back to 5.5 (Fig. 5B). For both resins, the shape and location of the Na^+ peaks is in excellent agreement with the conductivity traces (Fig. 2A and B).

The areas of both the negative and positive sodium ion peaks (Fig. 5A and B) were determined by numerical integration using

Table 3
Measured and calculated numbers of sodium ions exchanging on resin (N_{Na+}).

Resin	Negative peak (mmol)	Positive peak (mmol)	Predicted (mmol)
CM Ceramic HyperD	0.60	0.61	0.99
CM Sepharose FF	0.05	0.05	0.10

Table 4
Resin properties.

Resin	pK	Ligand density (mmol/L packed bed)
CM Ceramic HyperD	5.0	378
CM Sepharose FF	4.7	115

Simpson's rule (see Table 3). The areas of the negative and positive sodium ion peaks were in excellent agreement for both resins; this is consistent with the idea that equal numbers of counterions should exchange for pH shifts that are equal but opposite in magnitude. Based on the experimental results, approximately 12-fold more sodium ions exchange on CM Ceramic HyperD than on CM Sepharose for the pH shift from 5.5 to 7.5 with 100 mM MOPS.

Results of the resin titration analysis (Fig. 6) indicate that CM Ceramic HyperD does have higher intrinsic buffering capacity than CM Sepharose FF. The ligand density (q_R) of CM Ceramic HyperD is more than three times that of CM Sepharose FF (see Table 4). The measured ligand densities are in very good agreement with published manufacturer estimates of >250 and 90–130 meq/L for CM Ceramic HyperD and CM Sepharose, respectively [21,23]. Based on the measured pK values, a lower fraction of CM Ceramic HyperD ligands would be deprotonated relative to CM Sepharose FF at an equivalent pH (see Table 4). This is also consistent with the observation that many more sodium ions exchange on CM Ceramic HyperD than on CM Sepharose during the transition from pH 5.5 to 7.5 (see Table 3). Theoretical predictions based on these resin characteristics and Eq. (4) suggest that approximately 10-fold more counterions should exchange on CM Ceramic HyperD than CM Sepharose FF for the pH shift from 5.5 to 7.5 with 100 mM MOPS (see Table 3).

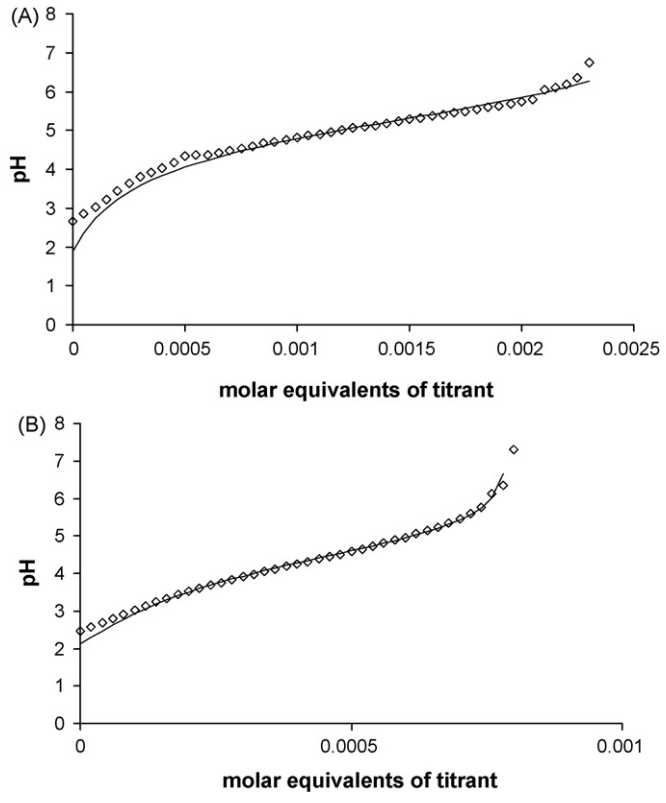

Fig. 6. Resin titration curves. Open symbols represent experimental data and the solid line represents the model fit to the data using parameters in Table 4. (A) CM Ceramic HyperD, (B) CM Sepharose FF.

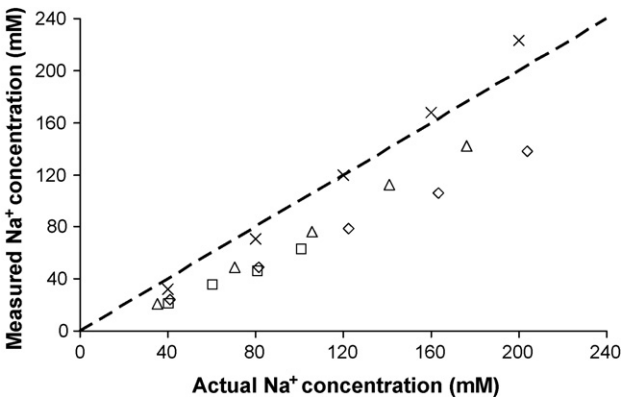

Fig. 7. Correlation plot for BioProfile 400 sodium ion concentration measurements in the presence of various anions. The dashed line represents ideal response of the analyzer. (◊) MOPS, pH 7.5, (□) MES, pH 5.5, (Δ) acetate, pH 5.5, (×) sodium chloride.

The number of counterions predicted to exchange (N_{Na+}) on CM Ceramic HyperD and CM Sepharose FF is greater than the experimental measurements by 62% and 100%, respectively (see Table 3). The most likely explanation for this discrepancy is inaccuracy in the experimental sodium ion concentration measurements. In each chromatographic experiment, the sodium ion concentrations in the high pH and low pH buffers were matched at 91 mM (see Table 1); however, the baselines of the experimental sodium ion concentration profiles were relatively flat at approximately 70 mM (see Fig. 5A and B). While experimental errors of this magnitude were not anticipated, additional testing with stock solutions of MOPS, MES, sodium acetate, and sodium chloride indicated that the accuracy of the BioProfile analyzer can be compromised by high concentrations of certain anions (see Fig. 7). In the case of MES and MOPS, the BioProfile analyzer significantly underestimated the concentration of sodium ions in solution. The magnitude of this error increased with the concentration of buffering species in solution. Somewhat smaller errors were observed for stock solutions of sodium acetate. The response of the BioProfile analyzer with respect to analyte concentration was much closer to ideal when the only ions in solution were Na^+ and Cl^-. The best results were obtained with NaCl at concentrations near that where the instrument was calibrated (140 mM). These observations suggest that the theoretical predictions may provide the most realistic estimates for the numbers of counterions exchanging (N_{Na+}) in this study.

4. Conclusions

High pH wash steps on weak cation exchange resins can be accompanied by significant conductivity fluctuations under commonplace operating conditions. The size of these conductivity transitions is directly related to the number of counterions exchanging onto or off of the resin during the pH shift. Factors that affect the number of counterions exchanging on the resin include resin ligand density and pK. In particular, increased ligand density leads to conductivity transitions of greater magnitude. Thus, the practical benefits associated with use of a high ligand density resin may require adoption of strategies to mitigate conductivity transitions.

One strategy employed successfully in this study was the use of a pH gradient in place of a stepwise change in pH. While this approach does not change the number of counterions that must exchange on the resin to shift the pH in the column, it results in broader, shallower conductivity transitions that can have dramatic effects on target protein retention. Here, the pH gradient was implemented with common buffers and very little optimization work. Overall, this approach could facilitate evaluation and optimization of chromatography on weak cation exchangers that provide high ligand density and high binding capacity such as CM Ceramic HyperD.

A commercial potentiometric electrode sensitive for sodium ions proved useful for following qualitative changes in the effluent counterion concentration during chromatography experiments. This technique could be used to help validate chromatography models that seek to predict pH and counterion concentration as a function of time, resin properties, and column feed composition. However, the accuracy of the electrode used here would first have to be improved before quantitative comparisons could be made with analytical models.

Ion exchange equilibrium theory was used to estimate the number of counterions expected to exchange on two different CM resins during a pH shift. The calculated results were consistent with the observation that many more counterions exchanged on CM Ceramic HyperD than on CM Sepharose FF for the pH shift of interest. As a practical matter, this approach could be used to guide the development of processes that involve weak cation exchange resins and pH shifts. For example, by selecting operating conditions and/or resins that minimize the number of exchanging counterions as predicted by Eq. (4), the process developer could reduce the amount of buffer consumed during pH shifts and decrease the likelihood of significant conductivity transitions. Such an approach should be relevant to column equilibration steps (such as those following regeneration and sanitization using sodium hydroxide) as well as high pH washes intended for impurity removal. Moreover, the relatively complicated resin titration experiments used in this study are likely not necessary if estimates for pK and q_R are available from the manufacturers of the resins of interest. Even a qualitative understanding of the relationship between resin properties, counterion exchange, and pH and conductivity transitions should benefit the rational design of weak cation exchange chromatography processes.

Acknowledgements

The authors would like to thank Tim Pabst, Jon Petrone, Warren Schwartz, Rob Fahrner, and Pat Rancatore for useful discussions.

The authors would like to thank Sujata Deshmane and Paul Liu for providing samples of CM Ceramic HyperD resin.

The authors would like to thank Veronica Carvalhal for guidance on the use of the BioProfile 400 analyzer.

References

[1] S.J. Sparham, E.R. Huehns, Hemoglobin 3 (1979) 13.
[2] Y. Fukami, Y. Hosaka, K. Yamamoto, FEBS Lett. 114 (1980) 342.
[3] C.R. Goward, G.B. Stevens, I.J. Collins, I.R. Wilkinson, M.D. Scawen, Enzyme Microb. Technol. 11 (1989) 810.
[4] S. Murao, Y. Nomura, K. Nagamatsu, K. Hirayama, M. Iwahara, T. Shin, Agric. Biol. Chem. Tokyo 55 (1991) 1739.
[5] C.Y. Tsao, F. Nagayama, J. Food Biochem. 15 (1991) 81.
[6] B.C. Baker, C.J. Campbell, C.J. Grinham, G. Turcatti, Biochem. J. 279 (1991) 775.
[7] Z.R. Gu, C.E. Glatz, Sep. Sci. Technol. 42 (2007) 1195.
[8] H. Tsukamoto, K. Fukudome, J. Kohara, H. Nakatake, M. Kimoto, Protein Expres. Purif. 56 (2007) 138.
[9] R. Necina, K. Amatschek, A. Jungbauer, Biotechnol. Bioeng. 60 (1998) 689.
[10] P. DePhillips, A.M. Lenhoff, J. Chromatogr. 933 (2001) 57.
[11] A. Staby, M.-B. Sand, R.G. Hansen, J.H. Jacobsen, L.A. Andersen, M. Gerstenberg, U.K. Bruus, I.H. Jensen, J. Chromatogr. 1069 (2005) 65.
[12] A. Staby, J.H. Jacobsen, R.G. Hansen, U.K. Bruus, I.H. Jensen, J. Chromatogr. 1118 (2006) 168.
[13] W.R. Melander, Z. El Rassi, C. Horvath, J. Chromatogr. 469 (1989) 3.
[14] W.-Y. Chen, Z.-C. Liu, P.-H. Lin, C.-I. Fang, S. Yamamoto, Sep. Purif. Technol. 54 (2007) 212.
[15] E. Karlsson, L. Ryden, J. Brewer, Protein Purification: Principles, in: High-Resolution Methods and Applications, Wiley-VCH, New York, 1998.
[16] S. Ghose, T.M. McNerney, B. Hubbard, Biotechnol. Prog. 18 (2002) 530.
[17] T.M. Pabst, G. Carta, J. Chromatogr. 1142 (2007) 19.
[18] J. Soto Perez, D.D. Frey, Biotechnol. Prog. 21 (2005) 902.
[19] T.M. Pabst, D. Antos, G. Carta, N. Ramasubramanyan, A.K. Hunter, J. Chromatogr. 1181 (2008) 83.
[20] F. Helfferich, Ion Exchange, McGraw-Hill, New York, 1962.
[21] Product Note, Q, S, DEAE, CM Ceramic HyperD Ion Exchange Sorbents, Pall Corporation Life Sciences, Port Washington, New York, 2004.
[22] L.E. Weaver, G. Carta, Biotechnol. Prog. 12 (1996) 342.
[23] GE Healthcare Data File, Sepharose Fast Flow Ion Exchangers, Uppsala, Sweden, 2003.